Solid-State Electronics Vol. 22, pp. 943–949
© Pergamon Press Ltd., 1979. Printed in Great Britain
0038–1101/79/0901–0943/$02.00/0

ONE-DIMENSIONAL DEVICE MODEL OF THE *npn* BIPOLAR TRANSISTOR INCLUDING HEAVY DOPING EFFECTS UNDER FERMI STATISTICS

AKIO NAKAGAWA
Toshiba Research and Development Center, 1, Komukai Toshiba-cho, Saiwai-ku, Kawasaki, 210, Japan

(*Received 7 December* 1978; *in revised form* 14 *April* 1979)

Abstract—Carrier transport equations extended to Fermi statistics will be given with characteristic parameters, including heavy doping effect. These equations will be solved numerically by introducing a new method for calculating the parameters. Calculated results will accurately reproduce the significant decrease in transistor current gain with a high impurity concentration at emitter-base junction.

NOTATION

- q unit charge
- ϵ dielectric constant of silicon
- k Boltzmann's constant
- T absolute temperature
- λ carrier screening length
- ρ_n, ρ_p total density of states functions for electron and hole
- $E_{\rm ion}$ parameter associated with ion screening
- E_{dn}, E_{dp} diffusion energies for electron and hole
- N_D, N_A donor and acceptor densities
- n_i, ω characteristic parameters: generalized electron-hole product, and a parameter related to the asymmetry of electrons and holes
- ω_n, ω_p another pair of characteristic parameters
- n_{io} electron-hole product in thermal equilibrium
- E independent energy variable. Positive direction is toward conduction band for electrons and toward valence band for holes
- F_n, F_p quasi-Fermi levels, measured from electrostatic potential toward conduction band for electrons and toward valence band for holes
- ϕ_n, ϕ_p quasi-Fermi levels for electron and hole
- $\phi_{n,E}, \phi_{p,B}$ quasi-Fermi levels for electron at emitter surface and for hole at base terminal
- ψ electrostatic potential
- n, p electron and hole densities
- J_n, J_p electron and hole current densities
- R recombination rate
- μ_n, μ_p electron and hole mobilities
- τ_n, τ_p carrier lifetimes for electron and hole
- α common base d.c. current gain
- α_s common base small signal current gain
- V_{BE}, V_{CE} base-emitter and collector-emitter voltages
- J_E, J_B, J_C emitter, base and collector current densities
- N_{SN} surface impurity concentration in emitter diffusion
- N_{SP} surface impurity concentration in base diffusion
- N_C impurity concentration at collector high resistivity region
- W_{NE} emitter width
- W_{PB} base width
- W_C collector high resistivity region width
- C_{EB} impurity concentration (N_D or N_A) at emitter-base junction.

1. INTRODUCTION

Recently, a large number of papers (e.g. [1, 2]) have been published regarding the decrease in the emitter efficiency of a bipolar transistor due to heavy doping effect. De Man[3] derived a modified formula, including position-dependent electron-hole ($p \cdot n$) product, for predicting the reduction in emitter efficiency, in accordance with the band gap decrease in a heavily doped emitter region, which had been proposed by Kaufmann and Bergh[4] and Buhanan[5]. Mertens, De Man and Overstraeten have shown, by using theoretically calculated $p \cdot n$ product[6], that the De Man's expression agrees with the experimental results[7]. Thus far, they all paid attention to the band gap decrease in heavily doped emitter region.

On the other hand, Mock[8, 9] solved a set of strict carrier transport equations for the emitter-base portion of a bipolar transistor under the Boltzmann statistics approximation, introducing carrier-dependent heavy doping parameters for the first time. A high base impurity doping, as well as a high emitter doping, was predicted to significantly reduce emitter efficiency. At the same time, it enhances the recombination current at the junction, causing an additional decrease in emitter efficiency at low injection levels.

Meanwhile, Azuma, Nakagawa and Takigami[10] have shown experimentally that a high impurity concentration at the emitter-base junction of a bipolar transistor, C_{EB}, leads to a drastic decrease in the transistor current gain.

In the present paper, Mock's transport equations will be extended to a general form written in terms of Fermi statistics to obtain more accurate results, introducing newly defined characteristic parameters. These parameters will be calculated efficiently by a new method described in Section 2. In Section 3, calculated results will be given about these parameters for various impurity concentrations, including excess carrier density variations. It will also be shown that Fermi statistics significantly reduce effective $p \cdot n$ product n_i when both excess carrier densities are above 10^{19}. In Section 4, calculated results about several high power transistors with high C_{EB} values will be shown to agree with experimental results, manifesting the validity of the C_{EB} value as a good parameter for predicting a significant reduction in the emitter efficiency due to heavy doping effects.

2. MATHEMATICAL MODEL

Basic equations, describing carrier behaviour in the semiconductor, are given under the assumption of quasi-equilibrium and Fermi statistics, as follows;

$$J_n = -qn\mu_n \frac{\partial \phi_n}{\partial x}, \quad (1)$$

$$J_p = -qp\mu_p \frac{\partial \phi_p}{\partial x}, \quad (2)$$

$$\frac{\partial J_n}{\partial x} = -\frac{\partial J_p}{\partial x} = qR, \quad (3)$$

$$\frac{\partial^2 \psi}{\partial x^2} = \frac{q}{\epsilon}(n - p + N_A - N_D), \quad (4)$$

$$n = \int_{-\infty}^{\infty} \rho_n(E, \lambda, N_D + N_A) \Big/ \left[1 + \exp\left(\frac{E - F_n}{\mathrm{kT}}\right)\right] \mathrm{d}E, \quad (5)$$

$$p = \int_{-\infty}^{\infty} \rho_p(E, \lambda, N_D + N_A) \Big/ \left[1 + \exp\left(\frac{E - F_p}{\mathrm{kT}}\right)\right] \mathrm{d}E. \quad (6)$$

Density of states functions $\rho_n(E)$ and $\rho_p(E)$ should reflect heavy doping effects. In the present paper, the same density of states function as that used in Ref. [8], was adopted because of its simplicity, being given as a function of E, $N_D + N_A$ and λ. The screening length λ for the quasi-equilibrium condition is assumed as,

$$\frac{\epsilon}{\lambda^2} = q^2\left[\frac{n}{E_{dn}} + \frac{p}{E_{dp}} + \frac{N_D + N_A}{E_{ion}}\right], \quad (7)$$

$$E_{dn} = \frac{n}{\dfrac{\partial n}{\partial F_n}}, \quad E_{dp} = \frac{p}{\dfrac{\partial p}{\partial F_p}}, \quad (8)$$

where E_{ion} is assumed to be 20 kT instead of 30 kT as given in reference [8] to give a better agreement with measured results as described in Section 4.

The Shockley–Read–Hall type recombination rate R and the impurity concentration dependent carrier lifetimes τ_n and τ_p are assumed as

$$R = \frac{p \cdot n - n_{io}^2}{\tau_n(p + n_{io}) + \tau_p(n + n_{io})}, \quad (9)$$

$$\frac{1}{\tau_n} = \frac{1}{\tau_p} = \frac{1}{\tau_1} + \frac{1}{\tau_2}, \quad (10)$$

$$\tau_2 = \tau_0 \cdot \frac{N_{ref}}{\mathrm{N_D + N_A}}, \quad (11)$$

where τ_1 is assumed to be a constant component attributed to crystal defects and lifetime killers. The measured carrier lifetime in the high resistivity collector region will be used as τ_1 for an approximation. The impurity concentration-dependent component τ_2 is assumed to be described by eqn (11) [11] in the present calculation. Electron and hole lifetimes τ_n and τ_p are given by eqn (10) by regarding the two contributions as independent. The τ_0 value will be determined to be 3 μsec with $N_{ref} = 10^{18}$ so as to obtain good agreement between theory and experiment in Section 4. This means that τ_2 takes on the reasonable value 3 μsec at $N_A + N_D = 10^{18}$, and will justify the present assumptions indirectly.

The field and impurity concentration dependent mobilities μ_n and μ_p are used, according to Scharfetter and Gummel [12].

Equations (1)–(8) have so many variables that it appears to be impractical to solve them directly. Instead, characteristic quantities ω_n and ω_p will be introduced in order to use conventional solution procedures, defined by the following eqns;

$$n = \int_{-\infty}^{\infty} \rho_n \frac{\mathrm{d}E}{1 + \exp\left(\dfrac{E - F_n}{\mathrm{kT}}\right)} \equiv n_0 \exp\frac{q}{\mathrm{kT}}\left[\frac{1}{q}F_n + \omega_n(F_n, \lambda, N_D + N_A)\right], \quad (12)$$

$$p = \int_{-\infty}^{\infty} \rho_p \frac{\mathrm{d}E}{1 + \exp\left(\dfrac{E - F_p}{\mathrm{kT}}\right)} \equiv n_0 \exp\frac{q}{\mathrm{kT}}\left[\frac{1}{q}F_p + \omega_p(F_p, \lambda, N_D + N_A)\right], \quad (13)$$

where n_0 is a given constant. ω_n and ω_p are the functions not only of λ and $N_D + N_A$ but also of F_n or F_p, thus including both the changes in the density of states functions and the discrepancy between Fermi statistics and Boltzmann statistics. The characteristic quantities n_i and ω will be redefined by

$$n_i \equiv n_0 \exp\frac{q}{\mathrm{kT}}((\omega_n + \omega_p)/2), \quad (14)$$

$$\omega \equiv (\omega_n - \omega_p)/2. \quad (15)$$

From eqns (1), (12), (2), (13), (14) and (15) and where $F_n = -q(\phi_n - \psi)$, $F_p = -q(\psi - \phi_p)$, the following equations are obtained.

$$n = n_i \exp\frac{q}{\mathrm{kT}}(\psi + \omega - \phi_n), \quad (16)$$

$$p = n_i \exp\frac{q}{\mathrm{kT}}(-\psi - \omega + \phi_p), \quad (17)$$

$$J_n = \mathrm{kT}\,\mu_n \frac{\partial n}{\partial x} - qn\mu_n \frac{\partial \psi_1}{\partial x}, \quad (18)$$

$$J_p = -\mathrm{kT}\,\mu_p \frac{\partial p}{\partial x} - qp\mu_p \frac{\partial \psi_2}{\partial x}, \quad (19)$$

$$\psi_1 = \psi + \omega + \frac{\mathrm{kT}}{q}\ln n_i, \quad (20)$$

$$\psi_2 = \psi + \omega - \frac{\mathrm{kT}}{q}\ln n_i. \quad (21)$$

Definitions (14) and (15) are based on the following fact. In eqns (20) and (21), ω behaves like ψ, whereas n_i

contributes in an opposite way to ψ_1 and ψ_2, so that it influences more significantly than ω. Parameter ω can be neglected to obtain approximated results, as will be shown in Appendix 1.

Equations (16)–(21) are similar to those given by Mock, except for the definitions of n_i and ω. However, it should be noted, in eqns (18) or (19) that the diffusion constant vs mobility ratio D_n/μ_n is not kT/q, but should be calculated from $(1/q)$ $[n/(\partial n/\partial F_n)]$. The product of $q \cdot D_n$ is not identical to the coefficient before $(\partial n/\partial x)$. In other words, these equations can be treated as if D/μ were apparently equal to kT/q, or as if these equations depended on Boltzmann statistics, once corresponding n_i and ω are obtained.

Equations (3), (4), (18)–(21) can be solved numerically by the usual Newton–Raphson iteration scheme (see, e.g.[13]) with recalculation of n_i and ω after each iteration. In Fermi statistics, recalculation of n_i and ω is not so easy as in the Boltzmann statistics approximation, because a set of eqns (5)–(8) and (12)–(15) have to be solved consistently for the corresponding electron and hole densities. Fortunately, it was found that the approximated λ can be used for the ρ_n and ρ_p calculation if the n_i and ω changes are small, realizing an efficient method to recalculate n_i and ω. The detailed solution procedure and the used boundary conditions for an *npn* transistor will be given in Appendix 2.

Summarizing the merit in the present method is that it includes both effects at the same time, thus reducing the required time to obtain calculation results.

3. n_i AND ω CALCULATED RESULTS WITH CARRIER DENSITY AS A PARAMETER

In this section, n_i and ω calculation results will be described in relation to carrier densities and Fermi statistics. The thermal equilibrium n_i and ω values for various impurity concentrations is almost the same as those calculated by Mock in Ref.[8] except for the E_{ion} value, thus not being repeated here.

Figures 1 and 2 are the results obtained under the conditions of $N_D = N_A$ and $n = p$, which are intended to simulate n_i and ω in the junction area. Figures 3 and 4 are the results obtained under conditions of $N_A = 0$ and $n = p + N_D$, which are intended to simulate n_i and ω in the quasi-neutral region. Hole density p can be regarded as the excess carrier density in both cases. In the junction area, n_i begins to decrease if the excess carrier density exceeds about $10^{15} \sim 10^{16}$, whereas n_i in the quasi-neutral region remains almost constant, unless the excess carrier density exceeds about $10^{17} \sim 10^{18}$. This fact is interpreted mainly by the change in the screening length. Equation (7) shows that λ changes almost according to $n + p$, if E_{dn} and E_{dp} are both assumed to be kT. In the junction area, λ begins to change if $n + p(=2p)$ approaches

$$\left(\frac{kT \cdot (N_D + N_A)}{E_{ion}}\right),$$

whereas, in the quasi-neutral region, λ does not change, unless $2p$ approaches N_D, which is always greater than

$$\left(\frac{kT \cdot (N_D + N_A)}{E_{ion}}\left(=\frac{N_D + N_A}{20}\right)\right)$$

in the present calculation. Thus, in a low emitter current

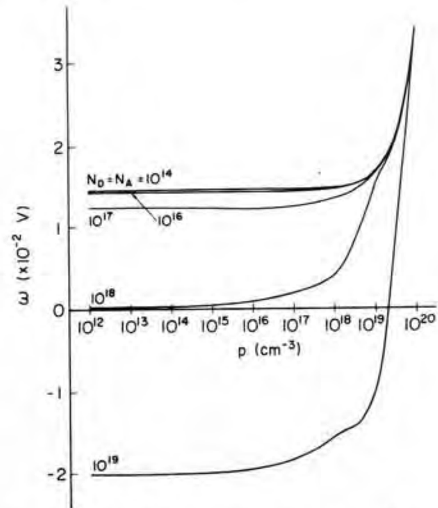

Fig. 2. ω vs hole density, when $N_A = N_D$ and $n = p$.

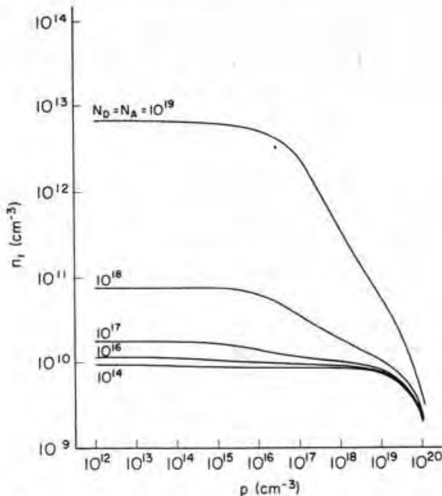

Fig. 1. n_i vs hole density, when $N_A = N_D$ and $n = p$.

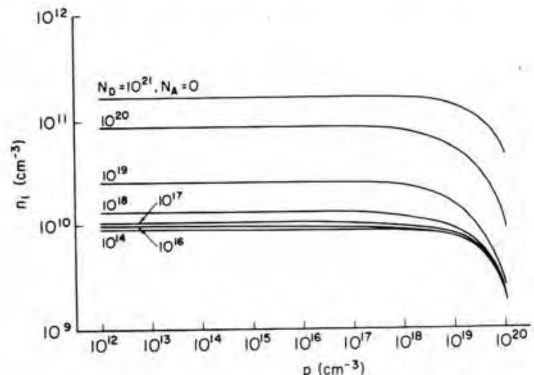

Fig. 3. n_i vs hole density, when $N_A = 0$ and $n = N_D + p$.

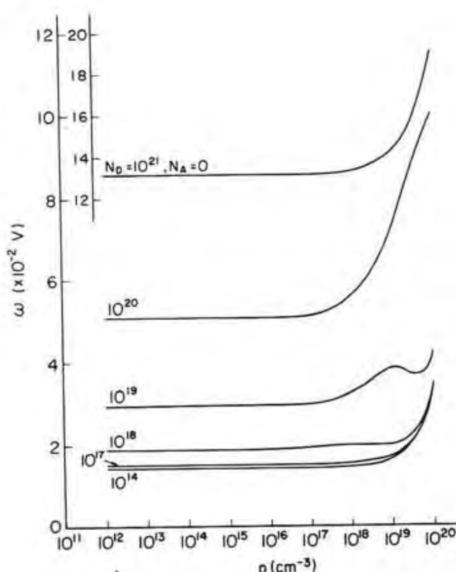

Fig. 4. ω vs hole density, when $N_A = 0$ and $n = N_D + p$. Curve, labeled $N_D = 10^{21}$, is plotted against the sub-scale.

condition, the change in n_i and ω in the junction area is important.

In Figs. 1 and 3, it is clearly seen that, for $p > 10^{19}$, n_i decreases drastically with an increase in p, regardless of the impurity level. This is caused by the application of Fermi statistics. When carrier density is greater than about 10^{18}, Fermi statistics generally give smaller carrier density than Boltzmann statistics for the same Fermi level, thus reducing n_i. If only Fermi statistics are taken into account, it follows that n_i decreases with an increase in the impurity concentration $|N_D - N_A|$, resulting in increasing the transistor current gain because of smaller n_i in the emitter region.

If we regard the difference of the value $[n/(\partial n/\partial F)]$ from kT as a measure of discrepancy from Boltzmann statistics, it follows that the application of Fermi statistics is necessary to calculate n_i and ω accurately in the region where either carrier density exceeds above $10^{18}/\text{cm}^3$.

In the high current region, where both excess carrier densities exceed 10^{19}, the effect of Fermi statistics becomes significantly important, reducing carrier densities as compared with Boltzmann statistics. For example, in a diode, the reduced number of carriers will cause a higher forward voltage drop than the results obtained under Boltzmann statistics.

4. CALCULATION RESULTS AND COMPARISON WITH EXPERIMENTAL RESULTS

In this section, the present device model will be applied to various mesa type diffused *npn* power transistor samples, with emphasis being laid on agreement between theory and experiment.

The samples, described in Table 1, were simultaneously fabricated through an identical number of processes. They were designed to have rather high base impurity doping to clearly reflect the heavy doping effect. The impurity profile used in the claculation was assumed to be Gaussian, and the surface concentration was determined from Irvin's curves. A lifetime τ_1 value of 10 μsec in the high resistivity collector region was measured by the diode voltage decay method. In eqn (11), impurity concentration dependent carrier lifetime constant τ_0 was assumed to be 3 μsec at $N_{ref} = 1 \times 10^{18}\,\text{cm}^{-3}$. These τ_1 and $\tau_0 \cdot N_{ref}$ values were kept constant, except for Fig. 9.

Figures 5–8 show calculated results on transistor *B*. In Fig. 5, the carrier distribution inside the device is demonstrated. It should be noted that the hole concentration in the emitter is fairly large, because of the large $p \cdot n$ product, n_i, as shown in Fig. 6. For $V_{BE} \gtrsim 0.83$, high excess carriers are seen to exist beyond the base-collector (B–C) junction in the high resistivity region. This is "base push-out effect". Returning to Fig. 6, one more noticeable point is the existence of a high n_i peak at the emitter-base (E–B) junction, which diminishes drastically with an increase in carrier density. The reason was already given in Section 2.

The calculated recombination rate R is shown in Fig. 7. The recombination rate clearly reflects the n_i distribution. Integration of R over the x axis yields the base current which amounts to a large value because of high R in the emitter region, thus resulting in a low current gain α over all current density levels. Recombination rate in the emitter and in the base neutral regions changes approximately proportionally to $\exp(qV_{BE}/kT)$, whereas it changes like $n_i \cdot \exp(qV_{BE}/2\,kT)$ in the E–B junction. Thus, as shown in Fig. 7, for lower V_{BE}, R at the

Table 1.

Samples	Emitter		Base		Collector	
	N_{SN} (cm^{-3})	W_{NE} (μm)	N_{SP} (cm^{-3})	W_{PB} (μm)	N_C (cm^{-3})	W_{NC} (μm)
A	2.5×10^{20}	15.0	2.2×10^{18}	42.0	1×10^{14}	200
B	2.5×10^{20}	15.4	2.66×10^{18}	39.8	2×10^{14}	150
C	5.5×10^{20}	10.2	2.12×10^{18}	45.8	2×10^{14}	150
D	4×10^{20}	11.6	2.75×10^{18}	41.9	2×10^{14}	150
E	5×10^{20}	9.2	2.8×10^{18}	43.3	2×10^{14}	150

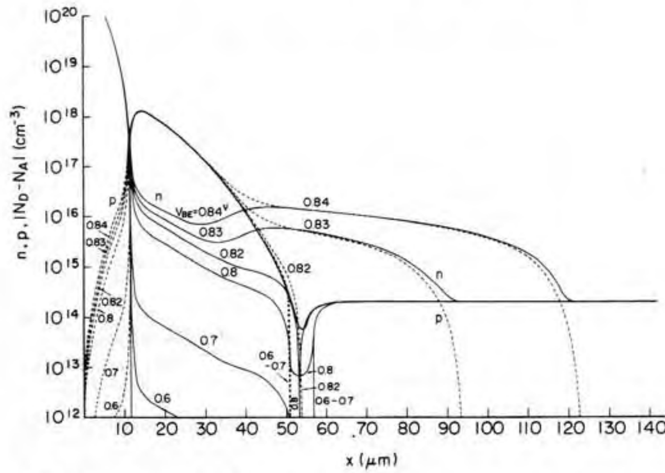

Fig. 5. Electron and hole distribution vs distance with V_{BE} as a parameter.

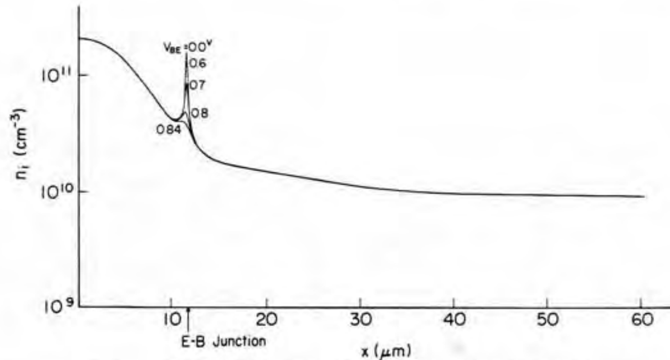

Fig. 6. n_i distribution vs distance with V_{BE} as a parameter.

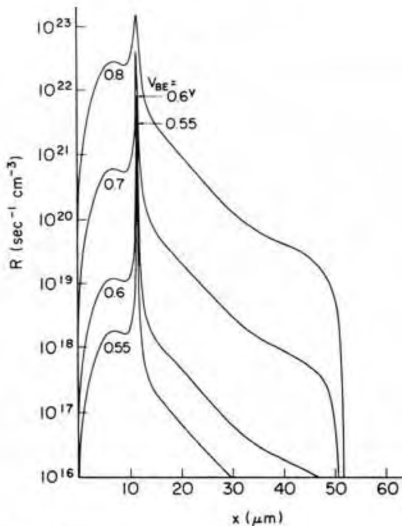

Fig. 7. Recombination rate vs distance with V_{BE} as a parameter.

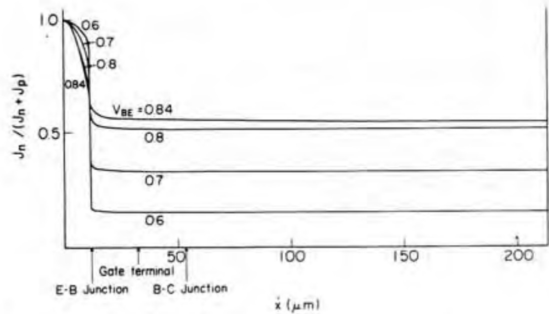

Fig. 8. Ratio $J_n/(J_n + J_p)$ vs distance with V_{BE} as a parameter.

junction is high, because of the increase in n_i corresponding to the decrease in carrier densities, thus giving rise to an accelerating current gain fall-off in lower current levels.

Figure 8 shows the rate of J_n to $J_n + J_p$ vs x distance for a number of emitter-base biases. It is clearly seen that the emitter efficiency mainly determines current gain α and that, especially for lower V_{BE}, the recombination of the E–B junction almost entirely determines the emitter efficiency.

The n_i in a highly compensated area, such as an E–B junction, depends clearly on the E_{ion} value, because the screening length λ is determined by the term $(N_D + N_A/E_{ion})$. A higher E_{ion} leads to a large n_i, thus decreasing the current gain through a large recombination at the junction. Figure 9 shows an example of calculated d.c. current gains of Tr. E for E_{ion} of 20 and 30 kT. The E_{ion} of 20 kT was used for all of the other results, so that the

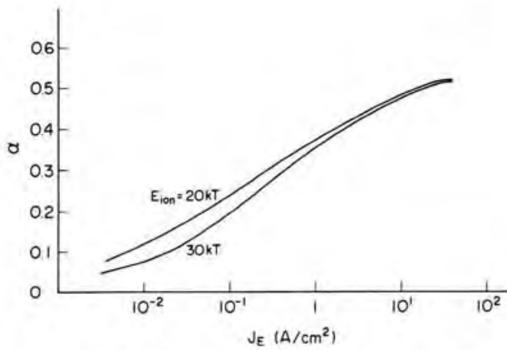

Fig. 9. Calculated d.c. current gain α vs emitter current with E_{ion} as a parameter and $V_{CE} = 5.0\,V$.

calculated results may be in better agreement with the experimental results.

Figure 10 shows calculated and measured small signal current gain vs emitter current characteristics for *Tr, B* and *D*. Alpha-reduction for $J_E > 20\ \text{A/cm}^2$ is due to the base push-out effect. Considering the number of approximations introduced to the adopted ρ_n and ρ_p expressions (see [8]) and a simple gaussian approximation for the impurity profile used in the calculation, the agreement between calculation and experimental results is considered to be satisfactory.

Figure 11 shows calculated small signal current gains for *Tr, A, B, C, D* and *E* at the emitter current of $0.5\ \text{A/cm}^2$, together with experimental results. Horizontal axis indicates the impurity concentration (N_D or N_A) at the *E–B* junction, C_{EB}, used in the calculation. The present model is able to fairly accurately reproduce a significant decrease in the current gain with increase in C_{EB}. The reduction in the current gain with increase in C_{EB} is caused mainly by (1) increase in n_i at junction region, (2) increase in the effective doping integration in the base region and (3) decrease in the effective doping integration in the emitter region.

The current gain reduction due to the C_{EB} value was experimentally confirmed in Ref. [10]. For example, in a gate-turn-off thyristor with a good current interruption capability, a high impurity concentration at a cathode-

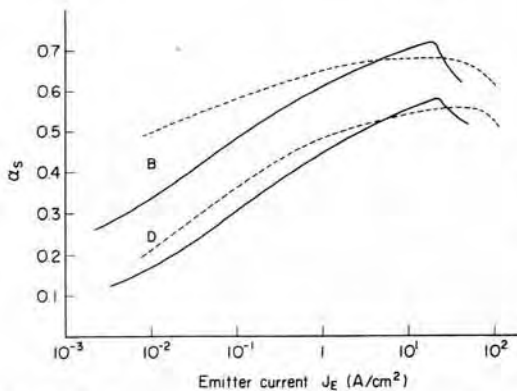

Fig. 10. Calculated small signal current gain vs emitter current with $V_{CE} = 5.0\,V$. Solid lines denote calculated values, while broken lines denote measured values.

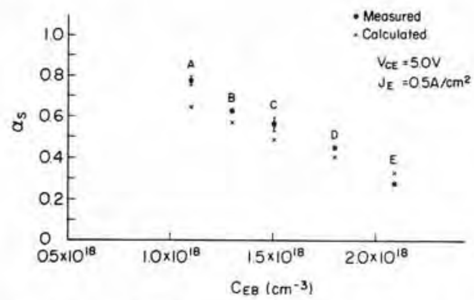

Fig. 11. Calculated and measured small signal current gain vs C_{EB} with $V_{CE} = 5.0\,V$ and $J_E = 0.5\ \text{A/cm}^2$.

gate junction is designed to retain low base sheet-resistance for achieving good current interruption capability. In this case, it was found empirically to be necessary to strictly control the impurity concentration at the junction for attaining high manufacturing yield, because it significantly influences the current gain of the three layers (cathode, gate and the other base layer). The present calculated results can interpret this empirical fact as a heavy doping effect.

It was found that in the present model the emitter surface impurity concentration N_{SN}, is not as influential on the current gain as the C_{EB} value. For example, the change in N_{SN} value from 1×10^{20} to 1×10^{21} for *Tr. E* causes only the change in current gain α_s from 0.29 to 0.36 at $J_E = 0.5\ \text{A/cm}^2$. This feature results from the fact that the effective doping $(N_D - N_A)/n_i^2$ does not change significantly with increase in N_D above $N_D > 1 \times 10^{20}$. Thus, it can be concluded, both theoretically and experimentally, that the C_{EB} value is a good parameter for predicting the current gain.

5. CONCLUSION

Extended carrier transport equations in Fermi statistics have been derived, including heavy doping effects. These equations were solved numerically by replacing n_i and ω, appropriately.

n_i and ω are characteristic quantities, including not only the changes in the density of states functions but also the discrepancy between Fermi statistics and Boltzmann statistics at the same time. They were shown to be calculated sufficiently efficiently by using the proposed procedure.

The calculated results for a number of bipolar transistor samples were shown to fairly accurately reproduce the current gain vs emitter current characteristics, as well as the significant decrease in the current gain corresponding to the increase in C_{EB}.

Acknowledgements—The author thanks Dr. M. Kurata for furnishing an opportunity to accomplish this work and Mr. M. Azuma for providing experimental data about transistors *B* and *D*.

REFERENCES

1. R. U. Martinelli and E. Jetter, *IEDM Technical Digest*, pp. 162–165 (1976).
2. H. C. de Graaff, J. W. Slotboom and A. Schmitz, *Solid-St. Electron.* **20**, 515 (1977).

3. H. J. De Man, *IEEE Trans. Electron. Dev.* **ED-18**, 833 (1971).
4. W. L. Kaufmann and A. A. Bergh, *IEEE Trans. Electron. Dev.* **ED-15**, 732 (1968).
5. D. Buhanan, *IEEE Trans. Electron. Dev.* **ED-16**, 117 (1969).
6. R. Van Overstraeten, H. J. de Man and R. Mertens, *IEEE Trans. Electron. Dev.* **ED-20**, 290 (1973).
7. R. Mertens, H. J. de Man and R. Van Overstraeten, *IEEE Trans. Electron. Dev.* **ED-20**, 772 (1973).
8. M. S. Mock, *Solid-St. Electron.* **16**, 1251 (1973).
9. M. S. Mock, *Solid-St. Electron.* **17**, 819 (1974).
10. M. Azuma, A. Nakagawa and K. Takigami, *Jap. J. Appl. Physics* **17**, Supplement 17-1, 275 (1977).
11. W. Anheier, W. L. Engl, O. Manck and A. Wieder, *IEDM Technical Digest*, pp. 363–366. Washington, D.C. (Dec. 1–3 1975).
12. D. L. Scharfetter and H. K. Gummel, *IEEE Trans. Electron. Dev.* **ED-16**, 64 (1969).
13. M. Kurata, *IEEE Trans. Electron. Dev.* **ED-19**, 1207 (1972).

APPENDIX 1

By denoting $\psi + \omega$ by Ψ, eqn (2) is rewritten as

$$\frac{\epsilon}{q}\frac{\partial^2\Psi}{\partial x^2} = n - p + \left(N_A - N_D + \frac{\epsilon}{q}\frac{\partial^2\omega}{\partial x^2}\right).$$

Since the magnitude of ω is in the order of $10^{-2}V$, as calculated in Section 3, the last term in the r.h.s. $(\epsilon/p)(\partial^2\omega/\partial x^2)$ can be neglected, compared with $N_A - N_D$, except at the junction. Through several calculated results, it was confirmed that neglect of ω is a good approximation, except for low injection levels. Thus the knowledge of only n_i will be sufficient for qualitative predictions.

APPENDIX 2

Boundary conditions for an npn *transistor*

At an ohmic contact, an infinite surface recombination rate is assumed, resulting in the following conditions.

$$p = p_0, \quad n = n_0,$$

where p_0 and n_0 are thermal equilibrium carrier densities calculated from eqns (5) to (8), with charge neutrality condition $n - p - N_D + N_A = 0$.

Another assumption will be made that, at the base terminal, the following relation holds:

$$\phi_{p,B} - \phi_{n,E} = V_{BE},$$

i.e. $p = n_i \exp(-\psi - \omega + V_{BE} + \phi_{n,E})$.

Solution procedure

The iteration will be carried out with recalculation of corresponding n_i and ω. The mth new value of $n_{i,m}$ and ω_m will be calculated by using Fermi levels ($F_{n,m-1}$, $F_{p,m-1}$), carrier densities (p_{m-1}, n_{m-1}) and diffusion energies ($E_{dn,m-1}$, $E_{dp,m-1}$) which will have been obtained in the $(m-1)$th iteration. The suffix m or $m-1$ shows that the quantity is associated with the mth or $(m-1)$th iteration. Approximated screening length λ_m, to be used for density of states functions ρ_n and ρ_p calculations, will be obtained by substituting n_{m-1}, p_{m-1}, $E_{dn,m-1}$ and $E_{dp,m-1}$ into eqn (7). Then, modified carrier densities n'_m, p'_m will be calculated numerically from eqns (5) and (6), with $F_n = F_{n,m-1}$, $F_p = F_{p,m-1}$ and $\lambda = \lambda_m$. Finally, the new values of $n_{i,m}$ and ω_m will be able to be obtained from eqns (12) to (15) by setting $n = n'_m$, $p = p'_m$, $F_n = F_{n,m-1}$ and $F_p = F_{p,m-1}$.

It will not be necessary to carry out n_i and ω recalculation after each iteration. Especially, in the early stage of calculation, it will be better to recalculate them after obtaining a certain degree of convergence for corresponding n, p and ψ. Recalculation of $n_{i,m}$ and ω_m will be terminated when modified carrier densities n'_m and p'_m become equal to n_{m-1} and p_{m-1} of the $(m-1)$th iteraction, respectively.